Available online at www.sciencedirect.com
SCIENCE DIRECT®
International Journal of Mass Spectrometry 243 (2005) 71–84
International Journal of Mass Spectrometry
www.elsevier.com/locate/ijms

A mass spectrometric study of glucose, sucrose, and fructose using an inductively coupled plasma and electrospray ionization

Vivien F. Taylor[a,*], Raymond E. March[b], Henry P. Longerich[c], Christopher J. Stadey[b]

[a] *Environmental and Resource Science, Trent University, 1600 West Bank Dr., Peterborough, Ont., Canada K9J 7B8*
[b] *Department of Chemistry, Trent University, Peterborough, Ont., Canada K9J 7B8*
[c] *Department of Earth Science and Centre for Earth Resources Research, Memorial University of Newfoundland, St. John's, NF, Canada A1B 3X5*

Received 8 November 2004; accepted 7 January 2005
Available online 30 January 2005

Abstract

Large polyatomic ions were observed in inductively coupled plasma mass spectra of solutions containing glucose, fructose, and sucrose, whereas mass spectra of solutions of acetic acid and ethanol obtained under similar operating conditions showed that these polyatomic ions were either totally absent or were observed at much lower intensities. These results suggest that sugar molecules, in particular, have an ability to survive the plasma, giving rise to polyatomic ions. Interferences on several isotopes were observed previously in a mass spectrometric study of diluted Canadian icewine; the interferences were attributed to the high sugar content in the solution, and not the ethanol content, demonstrating the need for careful consideration of the sample matrix for quantitative analysis. Product ion mass spectra of the sugar solutions were acquired by electrospray ionization tandem quadrupole time-of-flight mass spectrometry to better understand the composition and fragmentation of the sugar molecules. Fragmentation schemes for the formation of polyatomic ions from the sugar molecules and observed by inductively coupled plasma mass spectrometry (ICP-MS) are proposed.

Keywords: Polyatomic ions; Inductively coupled plasma mass spectrometry; Hot plasma; Gas phase acetic acid dimer; Sample matrix; Electrospray ionization mass spectrometry; Glucose; Fructose; Sucrose; Fragmentation; Icewine

1. Introduction

The origin of polyatomic ions in inductively coupled plasma mass spectrometry (ICP-MS) has been the source of some debate [1–5]. It was expected naively that the high temperature of the plasma should break all the molecular bonds producing atoms and ions. With such an ideal ion source, it was assumed that any polyatomic ions observed in ICP mass spectra were formed by recombination reactions of monoatomic ions and atoms in the plasma and expansion region, and that the formation of polyatomic ions was not affected by the chemical form of the elements in the sample, or rather the molecular composition of the sample matrix. The origin of polyatomic ions has been studied by several authors, but with mixed results [1,2]. A study of estimated and measured gas kinetic temperature in the ICP concluded that the origin of polyatomic ions depends on the ion and conditions during ion extraction, but that some oxide and argide species are present at greater abundances than would be expected in the plasma, suggesting that they are formed during the extraction process [2]. The formation of doubly charged oxide and hydroxide ions has also been attributed to reactions in the interface and ion optics region [3]. The influence of the chemical form of a molecular species in solution on polyatomic ion formation was first suggested by observations of the background spectral features of sulfuric acid solutions [4]. Further empirical evidence supporting the idea that the occurrence of polyatomic ions is related to the molecular composition of the sample was presented with the observation that clear differences exist in the ICP mass spectra of a solution of HCl compared with a solution

* Corresponding author. Tel.: +1 705 748 1011; fax: +1 705 748 1026.
E-mail address: vitaylor@trentu.ca (V.F. Taylor).

1387-3806/$ – see front matter © 2005 Elsevier B.V. All rights reserved.
doi:10.1016/j.ijms.2005.01.001

of $HClO_4$ having equimolar concentrations of H, O, and Cl [5].

In this study, high-resolution ICP-MS was used to identify large polyatomic ions in the mass spectra of solutions of glucose, fructose, and sucrose by their mass-to-charge ratio. These mass spectra were compared with ICP mass spectra of solutions of ethanol and acetic acid, containing nearly identical concentrations of C, H, and O as the sugar solutions, but in a different molecular form. In these solutions, the polyatomic ions observed in the sugar solutions were either absent or were present at very low intensities. This suggests that the presence of large polyatomic ions in the ICP mass spectra of sugar solutions can be attributed to an inadequate retention time in the plasma for rupture of all molecular bonds in these cyclic molecules.

Incomplete fragmentation of sugar molecules in the ICP was first suggested in a study of trace element concentrations in Canadian wines [6], in which large polyatomic ions were observed in late harvest and icewine samples, and interfered with trace element determination. Trace element composition of wines from various regions have been studied to fingerprint provenance, as wines made from grapes grown in a single geographical area will have trace element concentrations reflecting that local environment, as well as wine processing techniques [7–10]. Wines samples can be prepared for ICP-MS analysis by a simple dilution [7–12], which eliminates volatile element loss associated with digestion techniques [11], as well as improving cost and time efficiency as provenance studies require large numbers of samples. As well simple dilution procedures minimises reagent and laboratory contamination. Dilution of most table wines enables trace element determination, as ethanol content is reduced sufficiently to produce a stable plasma, and carbide interferences are sufficiently low for the determination of most elements [8,11,12]. In the earlier study, large polyatomic ions, attributed to sugar molecule fragments, were observed only in late harvest and icewines [6], which are produced from grapes left on the vine until late November, then picked and crushed frozen, giving them with a residual sugar content of greater than 125 g/L (reported as >35° Brix by winemakers) after fermentation, in which sugar is converted to CO_2. In the current study, the large polyatomic ions observed in the mass spectra of sugar solutions were also observed in a diluted icewine sample and caused significant interference with several elemental ions originating from the sample matrix. The presence of large polyatomic ions in samples with high sugar content demonstrates the need for careful consideration of sample matrix during quantitative elemental determination.

Electrospray ionization (ESI) tandem mass spectrometry, being a soft ionization technique, has been used to investigate the structure of saccharide molecules [13–16]. Product ion spectra differentiated 13 mono and disaccharides by both positive and negative ion ESI-MS/MS [13], and negative ion ESI-MS/MS has been used to study anionic adducts of glucose [14,15] and fructose [15]. Fragmentation of monosaccharide units was observed in underivatized oligosaccharides [16,17], as well as in heparin-derived polysaccharides [18,19]. Ring cleavage of small saccharide analogues of flavonoid glycosides was also reported [20–24], promoted by the increased stability of the glycoside bond by hydrogen bonding. The fragmentation of glucose, fructose, and sucrose molecules was examined by ESI-MS/MS, to explain further the formation of the most intense sugar fragments observed in the ICP-MS spectra.

2. Experimental

Solutions of 1 and 3% high purity D (−) fructose, D (+) glucose, and sucrose (Sigma–Aldrich, St. Louis), ethanol (VWR Canlab, Burlingon, Ont.) and glacial acetic acid (Mallinckrodt Chemicals, NJ) were prepared in 0.1 M HNO_3, made with ultra pure nitric acid (Fisher Optima) and 18 MΩ/cm^3 deionised water (Millipore, France) for ICP-MS analysis. Sugar solutions were analyzed by high-resolution ICP-MS (Element 2, ThermoFinnigan, Bremen), at "medium" resolution ($m/\Delta m = 4000$), with a high efficiency crossflow nebulizer (0.3 mL/min) and a Scott spray chamber. The instrument was operated with hot plasma conditions to promote atomization of the sample matrix, and the nebuliser gas flowrate was optimised for sensitivity accompanied by an acceptable low oxide formation; lowering the gas flowrate below that at which maximum sensitivity is obtained results in further lowering of the oxide (polyatomic ion) formation (Table 1). The instrument was re-optimised for solutions containing ethanol by adjusting the nebuliser gas flowrate to 0.90 L/min, from a flowrate of 0.93 used for all other solutions. An on-line internal standard containing Co, Rh, Tl, and Th was used for monitoring matrix effects; oxide formation as ThO^+/Th^+ was less than 5%. Mass accuracy was calculated using the internal standards and was better than 30 ppm. The instrument sensitivity under these conditions was 40,000 cps/ppb ^{115}In. Mass spectra were obtained in the range m/z 60–181, and each atomic mass unit was scanned in the range $m \pm 0.120$ amu, where m is an integer, to include all possible polyatomic ions, which can be identified by the mass defect.

For trace element determination in table wines, wine samples were diluted 1:1 with 0.1 M HNO_3 prior to analysis, to keep element concentrations well above detection limits but

Table 1
Instrumental parameters for ICP-MS analysis

Radiofrequency power (W)	1400
Nebulizer gas flow (L/min)	0.93
Auxiliary gas flow (L/min)	0.8
Cool gas flow (L/min)	16
Injection flowrate (mL/min)	0.3
Data acquisition	E-scan
Points per amu	50
Dwell time (ms)	100
# Scans	10
Locked mass isotope	$^{40}Ar^{40}Ar^+$
Scan range (m/z)	60–180

Table 2
Instrumental parameters for ESI-MS/MS analysis

Capillary voltage (kV)	3.0
Cone voltage (V)	30
Source block temperature (°C)	80
Desolvation gas temperature (°C)	150
Injection flowrate (μL/min)	10

to avoid plasma instability caused by introducing high concentrations of ethanol into the plasma [7–12]. In this study, a sample of icewine (Inniskillin Estate, Niagara, Ont.) was diluted 1:2 with 0.1 M HNO_3, to further reduce matrix effects due to the higher sugar content of the wine.

For the ESI-MS/MS analysis, 100 mg/L solutions of each of the sugars were prepared in 1:1 methanol:water. Product ion mass spectra were obtained on a Q-TOF 2 with a Z-spray ES source (Micromass, Manchester) in positive and negative modes for each of the sugars, using the molecular ion as the lock mass isotope, and collision energies of 4–30 eV. Instrumental parameters for the ESI-MS/MS analysis are given in Table 2.

3. Results and discussion

3.1. Identification of polyatomic ions in sugar solution by high-resolution ICP-MS

A high-resolution mass spectrum of a blank 0.1 M HNO_3 solution (Fig. 1) was compared with a 3% fructose ($C_6H_{12}O_6$) solution (Fig. 2), so as to distinguish between ions originating from the blank or from the instrument memory with those originating from the fructose solution. A narrow mass range, *m*/*z* 69–76, of the observed mass spectra is shown in each of Figs. 1 and 2. Polyatomic and elemental ions in the blank and sugar solutions were identified from their accurate mass/charge ratios. Ion signals due to polyatomic ions having the elemental composition $C_xH_yO_z^+$, which were observed in the fructose solution (Fig. 1), were completely absent from the blank solution (Fig. 2). All of the polyatomic ions observed in the range *m*/*z* 60–181 from the fructose solution are shown in Fig. 3(a–c). The abscissa in each of Fig. 3(a–c) is discontinuous such that only the upper part of each peak is shown so as to better illustrate the high mass resolution of the

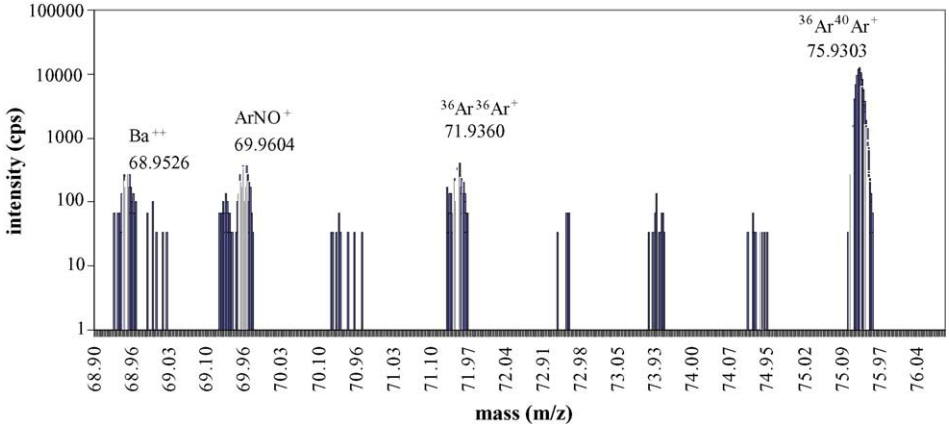

Fig. 1. High-resolution ICP mass spectrum of a blank 0.1 M HNO_3 solution over the mass range *m*/*z* 69–76.

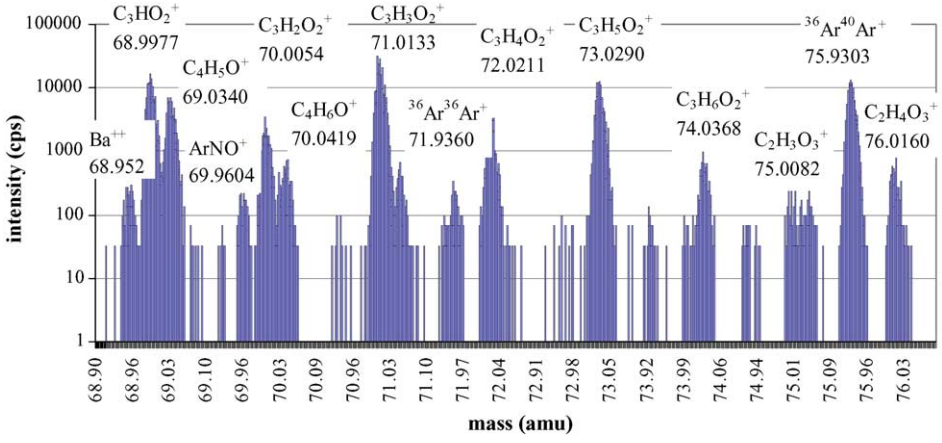

Fig. 2. High-resolution ICP mass spectrum of a 3% fructose solution over the mass range *m*/*z* 69–76.

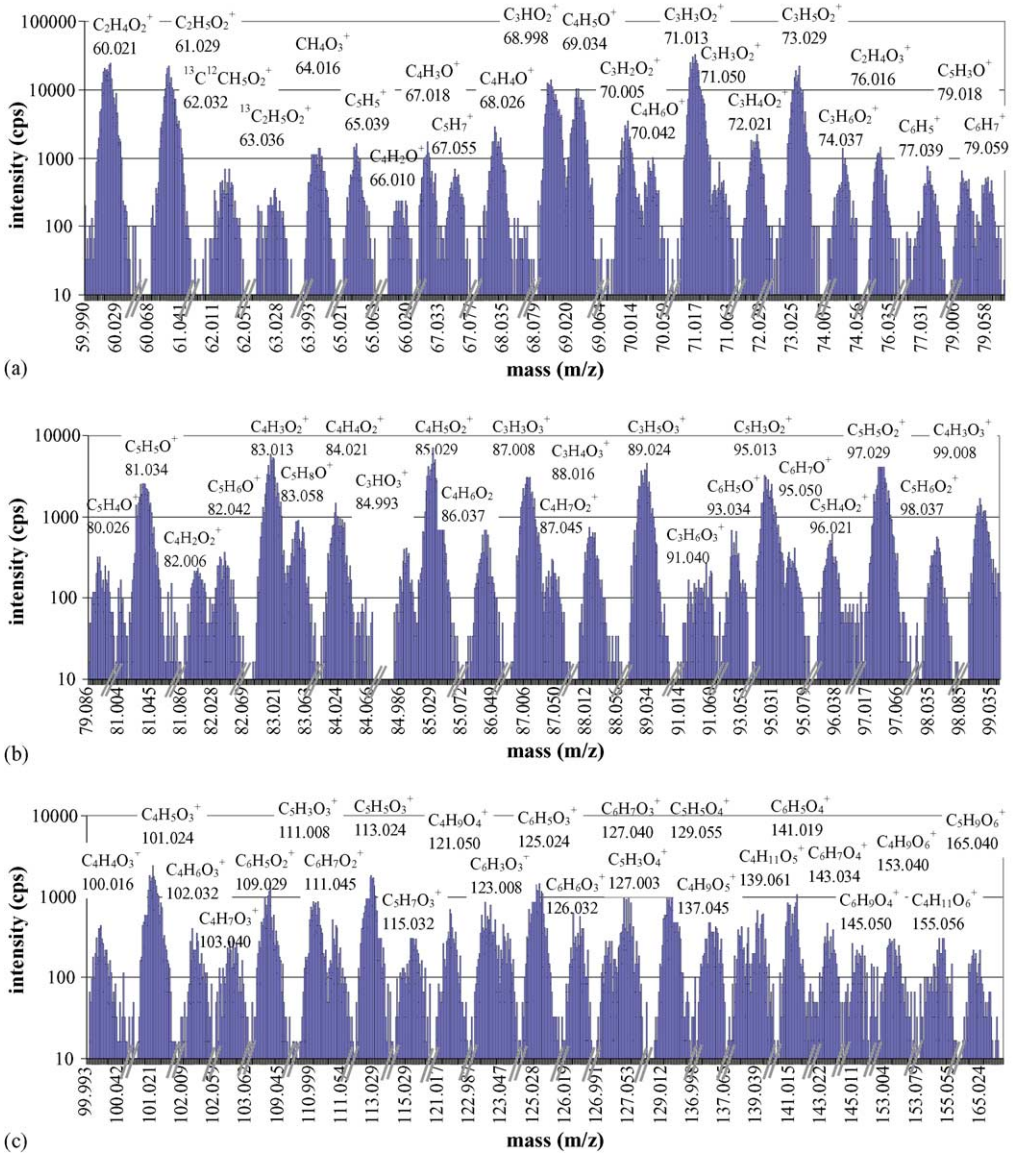

Fig. 3. Polyatomic ions observed in a high-resolution ICP mass spectrum of a 3% fructose solution: (a) mass range *m*/*z* 69–76; (b) mass range *m*/*z* 80–100; (c) mass range *m*/*z* 100–181.

data. ICP mass spectra obtained from solutions of 3% glucose ($C_6H_{12}O_6$) and 3% sucrose ($C_{12}H_{22}O_{11}$) were virtually identical to that of the fructose solution. In Table 3, the peak area of each of the organic polyatomic ions is tabulated along with the assigned $C_xH_yO_z^+$ formula of the ion, its calculated and observed masses, and the mass defect. The presence of these organic polyatomic ions in sugar solution mass spectra suggests strongly that sugar molecules are atomised incompletely in the ICP, and that the organic polyatomic ions are fragments of the sugar molecules in the sample.

To investigate further the relatively large organic ions observed in the mass spectra of sugars, 3% solutions of acetic acid and ethanol were examined by ICP-MS. The concentrations of C, H, and O atoms and the number of and type of chemical bonds in these solutions were similar to that contained in a 3% glucose solution. The ICP mass spectrum of a 3% acetic acid solution is shown in Fig. 4, in which very few ion signals were observed. The ion signals at *m*/*z* 60 and 61 are likely due to the molecular ion ($C_2H_4O_2$, MW: 60.021 Da) and the protonated molecule, respectively. The ion of *m*/*z* 69 may be explained by fragmentation of the acetic acid dimer that is stable in the gas phase. However, these ions and other ion species of *m*/*z* 70–76 are of much lower signal intensity than those observed in the mass spectra of the sugars. These polyatomic ions were not observed in the mass spectrum of the 3% ethanol solution.

In the mass spectrometric examination of five solutions containing similar concentrations of C, H, and O atoms and equal densities of chemical bonds, such as C–C, C–H, C–O, and O–H bonds, multiple polyatomic ions were observed

Table 3
Elemental compositions of positively-charged organic polyatomic ions identified from the ICP mass spectra of sugar solutions, along with their calculated masses, observed masses, mass error, 100% integrated peak area of polyatomic ions in 3% fructose, glucose, and sucrose solutions, and the mean and R.S.D. of the peak areas for all three sugars

Polyatomic ion formula	Calculated mass (Da)	Observed *m/z*	Error (mDa)	Error (ppm)	Fructose (cps)	Glucose (cps)	Sucrose (cps)	Mean (cps)	R.S.D. (%)
$C_2H_4O_2^+$	60.021	60.027	5	92	277144	550674	594336	474051	30
$C_2H_5O_2^+$	61.029	61.035	6	96	410192	426094	459293	431860	5
$^{13}CCH_5O_2^+$	62.032	62.036	4	63	11371	12667	12306	12115	5
$^{13}C_2H_5O_2^+$	63.036	63.031	5	77	6635	7567	5968	6723	10
$C_5H_5^+$	65.039	65.044	5	74	20787	32300	30735	27941	18
$C_4H_2O^+$	66.011	66.015	5	72	5568	6067	4600	5412	11
$C_4H_3O^+$	67.018	67.022	4	53	27397	24933	27831	26720	5
$C_5H_7^+$	67.055	67.059	4	64	9571	12733	15345	12550	19
$C_4H_4O^+$	68.026	68.029	3	39	45662	61900	54845	54136	12
$C_3HO_2^+$	68.998	69.001	3	42	358575	372339	335360	355425	4
$C_4H_5O^+$	69.034	69.037	3	40	170464	229476	230684	210208	13
$C_3H_2O_2^+$	70.005	70.007	2	24	62427	66633	60790	63283	4
$C_4H_6O^+$	70.042	70.042	<1	4	11441	17200	17181	15274	18
$C_3H_3O_2^+$	71.013	71.015	2	27	593374	846354	742711	727480	14
$C_4H_7O^+$	71.050	71.052	3	36	9039	7700	12140	9626	19
$C_3H_4O_2^+$	72.021	72.021	<1	4	87607	50133	48566	62102	29
$C_3H_5O_2^+$	73.029	73.030	1	16	275475	424132	435610	378406	19
$C_3H_6O_2^+$	74.037	74.034	2	33	16013	19767	16780	17520	9
$C_2H_4O_3^+$	76.016	76.016	<1	1	13408	26667	29100	23058	30
$C_6H_5^+$	77.039	77.039	<1	5	10536	17867	14439	14281	21
$C_5H_3O^+$	79.018	79.019	<1	7	13805	14700	14054	14186	3
$C_6H_7^+$	79.055	79.055	<1	8	9569	12300	11587	11152	10
$C_5H_4O^+$	80.026	80.026	<1	8	6734	9067	7902	7901	12
$C_5H_5O^+$	81.034	81.035	<1	10	77086	93200	93415	87900	9
$C_4H_2O_2^+$	82.006	82.004	1	16	5700	8200	7851	7250	15
$C_5H_6O^+$	82.042	82.040	2	19	7951	10867	11822	10213	16
$C_4H_3O_2^+$	83.013	83.013	<1	0	127078	148136	132221	135812	7
$C_5H_7O^+$	83.058	83.050	8	95	20198	17600	16943	18247	8
$C_4H_4O_2^+$	84.021	84.020	<1	10	31466	38400	39647	36504	10
$C_3HO_3^+$	84.993	84.991	1	16	7802	12400	10470	10224	18
$C_4H_5O_2^+$	85.029	85.028	<1	10	125008	139302	113287	125866	8
$C_4H_6O_2^+$	86.037	86.034	3	34	11921	13400	10219	11847	11
$C_3H_3O_3^+$	87.008	87.007	2	17	80089	85300	107490	90960	13
$C_4H_7O_2^+$	87.045	87.041	3	36	5084	4767	4617	4823	4
$C_3H_4O_3^+$	88.016	88.013	3	34	16209	14700	14174	15028	6
$C_3H_5O_3^+$	89.024	89.022	1	16	102129	97367	85431	94976	7
$C_3H_7O_3^+$	91.040	91.041	1	11	4917	3333	3050	3767	22
$C_6H_5O^+$	93.034	93.033	<1	5	10820	10767	10537	10708	1
$C_5H_3O_2^+$	95.013	95.014	<1	2	75597	67400	63825	68941	7
$C_6H_7O^+$	95.050	95.049	1	11	8951	12900	10637	10829	15
$C_5H_4O_2^+$	96.021	96.021	<1	4	12421	13000	13287	12903	3
$C_5H_5O_2^+$	97.029	97.029	<1	4	123920	114667	112181	116923	4
$C_5H_6O_2^+$	98.037	98.032	5	54	11503	11833	18052	13796	22
$C_4H_3O_3^+$	99.008	99.006	2	17	39481	45000	40282	41588	6
$C_4H_4O_3^+$	100.016	100.014	2	20	10209	8741	8593	9181	8
$C_4H_5O_3^+$	101.024	101.024	<1	1	50670	47050	45689	47803	4
$C_4H_6O_3^+$	102.032	102.031	<1	7	6747	2554	2963	4088	46
$C_4H_7O_3^+$	103.040	103.040	<1	5	6363	7482	6843	6896	7
$C_6H_5O_2^+$	109.029	109.030	1	9	23913	24984	17395	22097	15
$C_5H_3O_3^+$	111.008	111.007	1	11	21198	20378	29872	23816	18
$C_6H_7O_2^+$	111.045	111.042	3	23	7362	7623	9380	8122	11
$C_5H_5O_3^+$	113.024	113.023	1	8	44557	42978	49345	45627	6
$C_5H_7O_3^+$	115.032	115.036	4	35	6649	7236	6587	6824	4
$C_4H_9O_4^+$	121.050	121.034	1.6	129	10120	13920	12791	12277	13
$C_6H_3O_3^+$	123.008	123.016	7	60	16326	21354	20018	19233	11
$C_6H_5O_3^+$	125.024	125.030	6	47	37146	58615	44276	46679	19
$C_6H_6O_3^+$	126.032	126.036	4	35	9119	10887	8653	9553	10
$C_5H_3O_4^+$	127.003	127.007	4	28	7295	6801	7285	7127	3
$C_6H_7O_3^+$	127.040	127.044	5	38	15579	10972	9970	12174	20
$C_5H_5O_4^+$	129.019	129.024	5	38	26009	39616	42639	36088	20

Table 3 (*Continued*)

Polyatomic ion formula	Calculated mass (Da)	Observed *m/z*	Error (mDa)	Error (ppm)	Fructose (cps)	Glucose (cps)	Sucrose (cps)	Mean (cps)	R.S.D. (%)
$C_4H_9O_5^+$	137.045	137.029	1.6	114	11872	15257	12771	13300	11
$C_4H_{11}O_5^+$	139.061	139.037	12	86	10238	9553	10320	10037	3
$C_6H_5O_4^+$	141.019	141.017	2	12	19085	21653	16212	18983	12
$C_6H_7O_4^+$	143.034	143.034	<1	4	6885	6934	5050	6290	14
$C_6H_9O_4^+$	145.050	145.015	34	236	4550	5400	6218	5389	13
$C_4H_9O_6^+$	153.040	153.016	23	151	6484	9653	7953	8030	16
$C_4H_{11}O_6^+$	155.056	155.030	21	136	5384	4434	3700	4506	15
$C_5H_9O_6^+$	165.040	165.004	35	211	4334	4417	4334	4362	1

only in the mass spectra of the sugar solutions, providing evidence that the observed species were produced by incomplete atomization and not recombination or clustering reactions in the plasma or expansion region of the ICP-MS. A contributing factor to the incomplete atomization of the sugar molecules may be the higher vapour pressures of acetic acid and ethanol than the aqueous sugar solutions, such that more of these compounds will be transported from the spray chamber to the plasma as vapours than droplets. Droplets have been shown to desolvate to produce particles in the plasma, which are then vapourised [25,26] prior to atomization and ionization; molecules that reach the plasma in droplets may not have sufficient retention time to achieve complete atomization compared with those in the vapour phase. A principal difference between the solutes examined lies in the types of structures assumed by the solutes; the sugars have a ring structure while acetic acid and ethanol have linear structures, except in the gas phase where acetic acid forms a stable ring-shaped dimer. Thus, it would appear that the molecular structure of the solute is a determining factor in the extent of chemical bond rupture in a molecule in an inductively coupled plasma. While the high temperature of the plasma, estimated to be >5000 K [2], should provide sufficient energy to break all chemical bonds, the short residence time of sample molecules in the plasma enables, clusters of strongly bonded atoms to remain intact and become ionized. The ring structures of the sugar molecules, compared with the smaller linear molecules, will have greater enthalpies of formation and will require a greater acquisition of energy in order to be completely atomized.

3.2. High-resolution ICP mass spectra of an icewine sample

A sample of icewine diluted 1:2, such that it has an ethanol concentration of 3.5%, contains equal amounts of glucose and fructose [27] for a total concentration of >4%. A high-resolution ICP mass spectrum of the sample, in the mass range *m/z* 60–180, showed that several elemental metal isotopes in the wine were subjected to interference by polyatomic ions (Fig. 5). The high carbon content of the icewine due to both sugar and ethanol caused carbide interferences on some elemental isotopes; for example, the elemental ions, $^{60}Ni^+$ and $^{61}Ni^+$ suffered interference from TiC^+ and CaC^+. Furthermore, $^{60}Ni^+$, $^{61}Ni^+$, and the monoisotopic elements ^{75}As and ^{111}Cd suffered interference from organic polyatomic ions of elemental composition $C_xH_yO_z^+$. Such interference for ^{111}Cd is vexatious because this is the only isotope of Cd free from interference from other elemental isobaric ions.

The organic polyatomic ions in the icewine mass spectrum arise from the high sugar content of the icewine, and not from the ethanol content. It is important, therefore, for quantitative analysis of icewines and other samples with high sugar content that the samples be matrix matched to blanks and standards by their sugar concentration, particularly when a low resolution ICP-MS instrument is used. In trace element studies, wine samples are typically diluted and blanks and standards are matrix matched to the ethanol content of the wine [7–9,28] but it is apparent that, in some cases, the sugar

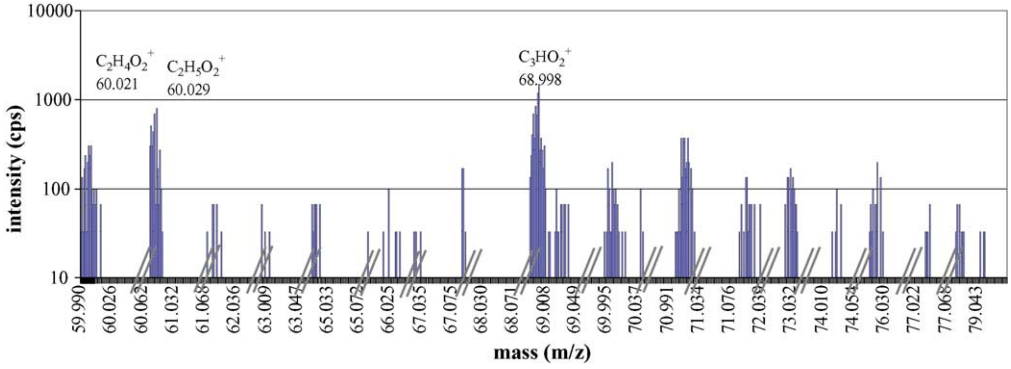

Fig. 4. Polyatomic ions observed in a high-resolution ICP mass spectrum of a 3% acetic acid solution over the mass range *m/z* 60–181.

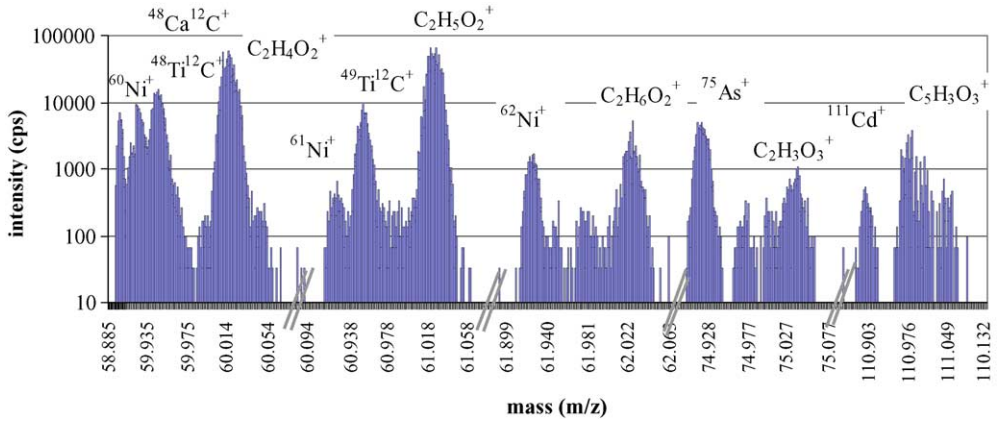

Fig. 5. Diatomic and organic polyatomic ion interferences with the isotopes $^{60}Ni^+$, $^{61}Ni^+$, $^{62}Ni^+$, $^{75}As^+$, and $^{111}Cd^+$.

content of the wine should also be considered for accurate determination of elements.

The application of high-resolution ICP-MS to resolve elemental ions from large polyatomic interferences originating from the sample matrix is demonstrated in Fig. 5. Other instrumental techniques that could be applied to the reduction of carbon-based polyatomic ions include the use of an inert gas in a collision cell ICP-MS [29], or by use of mixed oxygen–argon plasma, to oxidize carbon, which in turn may reduce the intensity of some organic polyatomic ions [30,31].

3.3. ESI-MS/MS study of sugar fragmentation

Mass spectra of glucose, fructose, and sucrose solutions were acquired by ESI-MS/MS, in both positive and negative ion mode. Product ion mass spectra of $[M-H]^-$ from solutions of all three sugars yielded more fragmentation products than did those from $[M+H]^+$, where M represents a sugar molecule; a distinctive fragmentation pattern was observed from each of the sugar solutions. Electrospray MS studies of oligosaccharides in negative ion mode are advantageous because of the low level of formation of cationic adducts with ubiquitous ions such as Na^+ [16]; in positive ion mode, these adducts deteriorate the signal from the protonated molecule. Inductively coupled plasma MS is typically only operated in positive ion mode, as high negative ionization potentials of most elements preclude significant ionization in the plasma. For this reason most ICP-MS instruments are built with lenses for positive ion transmission only. Each product ion mass spectrum was obtained at constant collision gas pressure and at a collision energy corresponding to a decrease in signal intensity of 30% for the precursor ion. These conditions yielded the maximum number of product ions.

The product ion mass spectrum of $[M-H]^-$ from fructose, at a collision energy of 8 eV, is shown in Fig. 6; nine fragment ions having a signal intensity of $\geq$10% of the precursor ion were observed. With the exception of the ion of m/z 87, the fragment ions are formed by multiple losses of H_2O and/or CH_2O from the deprotonated molecule, each loss being an endothermic reaction having a relatively low energy

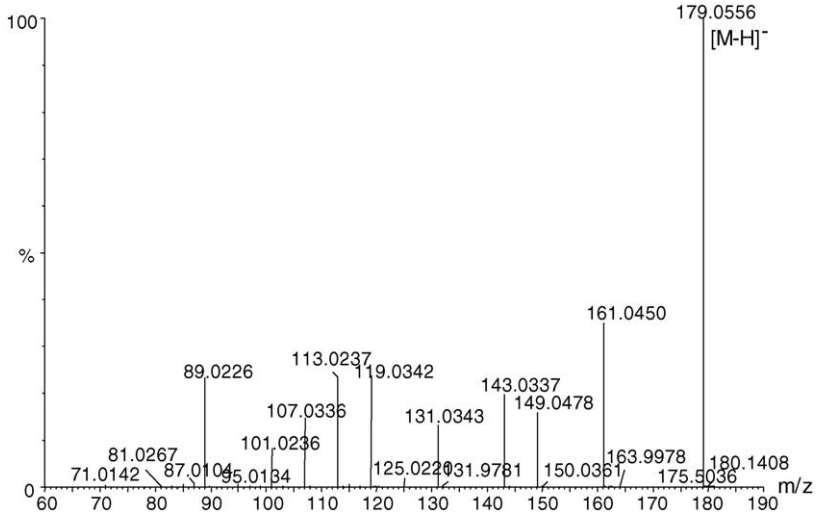

Fig. 6. ESI-MS/MS product ion mass spectrum of $[M-H]^-$ of fructose observed at a collision energy of 8 eV.

of activation. The formation of *m*/*z* 87 is of particular interest, as it is believed to be formed by oxidation of *m*/*z* 89 by loss of H_2; the formation of *m*/*z* 87 is the sole instance of oxidative dissociation observed in this ESI-MS/MS study. At a laboratory collision energy (E_{lab}) of 8 eV, the collision energy in the center-of-mass frame (E_{cm}) from a collision with argon atoms is 1.5 eV. While multiple collisions of the precursor ion with argon atoms will occur when the precursor ion signal intensity is reduced by 30%, the additional acquisition of energy by the precursor ion after the first collision will be small because the E_{cm} will be <1.5 eV. As E_{cm} is increased, so is the mass of the neutral fragment lost from the precursor ion.

Proposed fragmentation pathways and structures of the product ions observed in Fig. 6 are given in Scheme 1, in which the step-by-step fragmentation of the precursor ion is depicted as would be expected from a series of mass spectra recorded at increasing E_{cm}. There are several choices for the loss of the first molecule from $[M-H]^-$ from fructose, which loses 1–4 H_2O molecules and 1–3 CH_2O molecules. An attempt has been made to propose a reasonable sequence of fragmentation steps and fragment ion structures cognisant of the requirements for elemental composition and chemical valency. It is noted that cleavage and/or contraction of the furan ring has been invoked in proposing the structures of the product ions $m/z \leq 95$. Two configurations of the ion at *m*/*z* 125 are proposed: the 4-membered ring, which undergoes facile loss of CH_2O to form the ion at *m*/*z* 95, and the 5-membered ring species which undergoes ring cleavage, accompanied by migration of the negative charge, to form the primary alcohol at *m*/*z* 107.

In the product ion mass spectrum of $[M-H]^-$ from glucose obtained at $E_{cm} = 0.7$ eV ($E_{lab} = 4$ eV) and shown in Fig. 7, five fragment ions having a signal intensity of ≥5% of the precursor ion were observed; these fragment ions were formed by neutral losses of formaldehyde or water. The three dominant fragment ions at $E_{cm} = 0.7$ eV corresponded to the losses of 1–2 H_2O molecules and a CH_2O molecule. Proposed structures for the fragment ions are shown in Scheme 2. It is recognised that even for the primary fragment ions, there are several possible structures; for example, the loss of a CH_2O molecule to form the ion of *m*/*z* 149 may occur at C1–C4 and

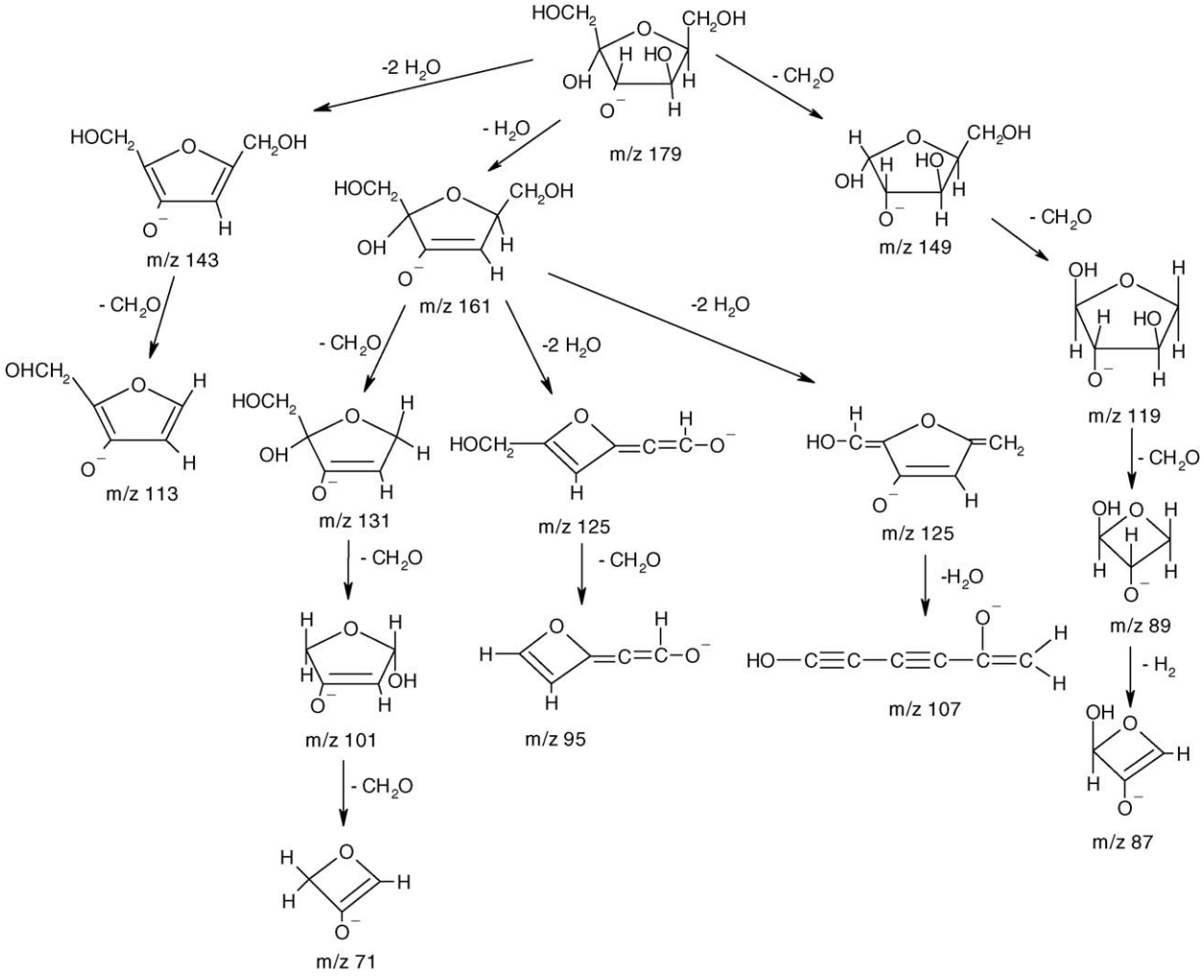

Scheme 1. Proposed structures for product ions of $[M-H]^-$ of fructose observed by ESI-MS/MS.

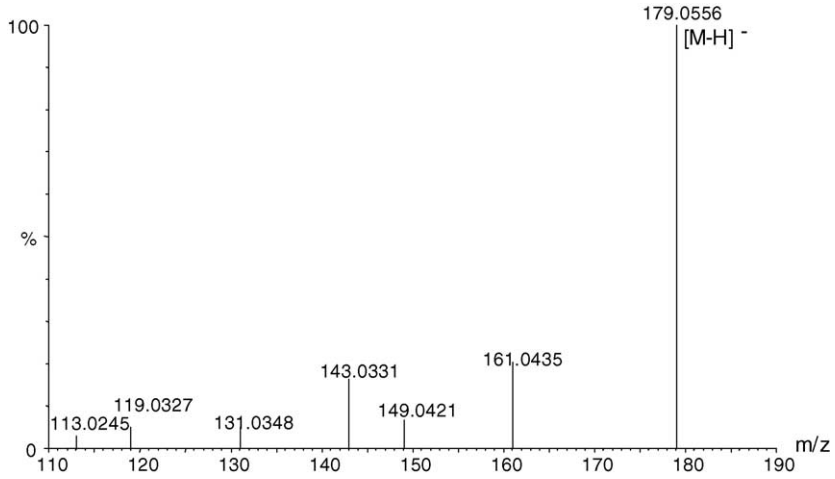

Fig. 7. ESI-MS/MS product ion mass spectrum of $[M-H]^-$ of glucose observed at a collision energy of 4 eV.

give rise to stereoisomers that differ with respect to orientation of hydroxyl groups. In addition, a CH_2O group may be lost at C6 attached to the ring, although the C5–C6 bond may be stronger than ring C–C bonds and will not break prior to formation of a 5-membered ring. Similarly, dehydration may occur at five possible places in the molecular ion, although only one structure is shown in Scheme 2.

The product ion mass spectrum of $[M-H]^-$ from sucrose, a disaccharide, at $E_{cm} = 2.1$ eV ($E_{lab} = 20$ eV) and shown in Fig. 8 reveals six fragment ions having a signal intensity of $\geq$10% of the precursor ion. The ions at *m/z* 179 and 161 indicate scission of the glycoside bond to form the complementary ions [glucose – H]$^-$ or [fructose – H]$^-$ and [glucose – H_3O]$^-$ or [fructose – H_3O]$^-$. The other four product ions, at *m/z* 119, 131, 143, and 149, and which were present in the product ion mass spectrum of $[M-H]^-$ from each of glucose and fructose, are formed by neutral losses of H_2O and CH_2O.

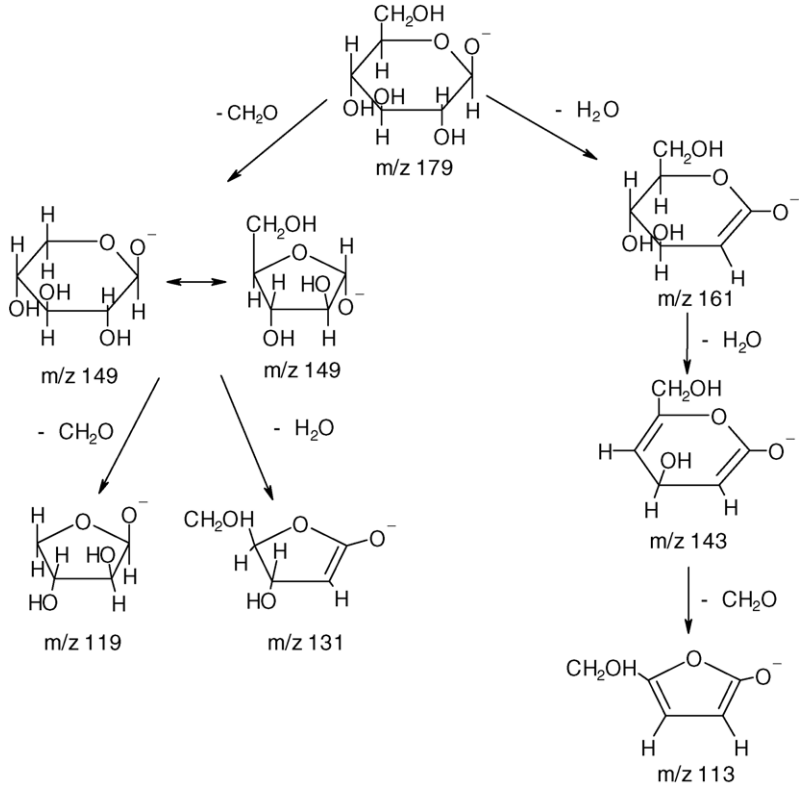

Scheme 2. Proposed structures for product ions of $[M-H]^-$ of glucose observed by ESI-MS/MS.

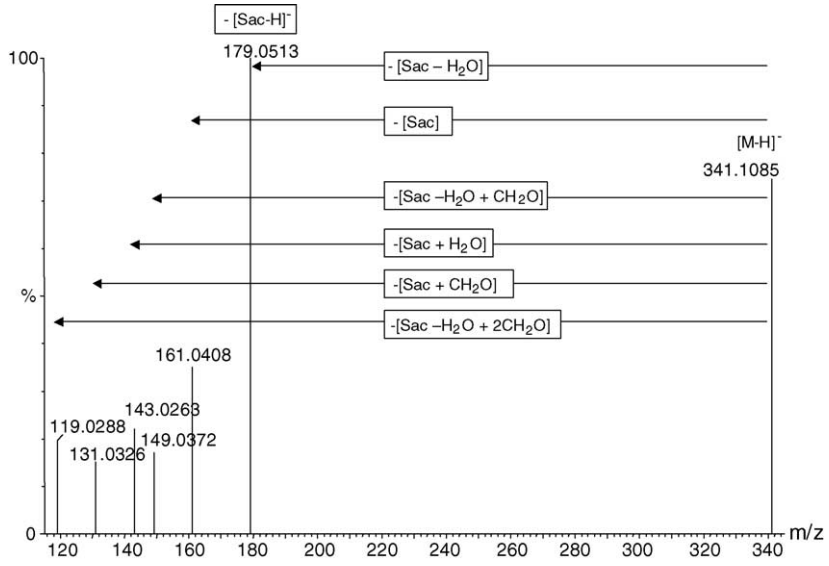

Fig. 8. ESI-MS/MS product ion mass spectrum of $[M-H]^-$ of sucrose observed at a collision energy of 20 eV.

3.4. Sugar fragmentation in the ICP

While the elemental composition of the polyatomic ions observed by high-resolution ICP-MS can be determined, in many cases, from the experimental mass/charge ratio, the formation and structures of the polyatomic ions observed are somewhat speculative even when based on the known structure of the precursor and general chemical intuition. Comparison of positive ion mass spectra obtained by ICP-MS with product ion mass spectra of deprotonated sugar molecules obtained by ESI-MS/MS is readily justified. The losses of 1–4 H_2O molecules and of 1–3 CH_2O molecules from deprotonated molecules have similar energy requirements to those losses from a protonated molecule; that is, the neutral moieties lost are the same regardless of precursor ion polarity. Thus, in a comparison of positive ion ICP mass spectra with ESI mass spectra obtained from deprotonated sugar molecules, the neutral moieties lost must be considered.

ESI-MS/MS is restricted usually to "gentle" or low E_{cm} energy fragmentation in 1–3 collisions that is associated with ion rearrangement rather than scission processes. Scission processes generally require higher activation energies than do rearrangement processes and, as such, scission processes will be favoured in ICP-MS. The higher energy of an inductively coupled plasma and greater collision number within the ICP source will promote more bond breakages and, given a residence time of sufficient duration, will result in formation of fragment ions of lower mass/charge ratio than those observed in ESI mass spectra.

Unlike the ESI-MS/MS mass spectra of the sugar solutions, the deprotonated molecules of fructose and glucose (*m*/*z* 179) were not observed in the ICP mass spectra, and deprotonated sucrose (*m*/*z* 341) was out of the mass range of the instrument. The absence of the protonated molecules indicates that all sugar molecules have undergone some fragmentation. The large variety of polyatomic ions shown in Fig. 3 suggests that numerous fragmentation pathways are accessed due to the high energy of the inductively coupled plasma. Formation of those organic ions observed at the highest intensities (>25,000 cps) is discussed in detail.

Examination of the organic polyatomic ions in the ICP mass spectrum of fructose (Fig. 3(a–c); Table 3) reveals that cations having odd mass/charge ratios are far more numerous in the mass spectrum than are ions that have even mass/charge ratios. Given that the sugar molecules have an even molecular mass, and most neutral losses from hydrocarbon molecules in mass spectrometry are also of even mass (H_2O, CH_2O, and CO_2) it is suggested that the sugar molecules are protonated in the acidic solution, which was aspirated into the plasma. Proton affinities of the ethanol, acetic acid, and glucose are 803.4 kJ/mol, 783.7 kJ/mol [32], and 1620 kJ/mol, respectively [33], and the protonated molecules are more stable than the free molecules in the gas phase. It is also observed that the ions of even mass are of too high relative abundance to the peak at (*m*/*z* −1), to be due to the ^{13}C isotope, with an isotopic abundance of 1.1%, and are therefore radical cations. The only exception may be the moieties at *m*/*z* 62 and 63, the intensities of which are 3.4 and 2.1% of the intensity of $C_2H_5O_2^+$ at *m*/*z* 61. The ^{13}C isotopic abundance of this ion is 2.2% at $^{13}C^{12}CH_5O_2^+$ (*m*/*z* 62) and 1.1% at $^{13}C_2H_5O_2^+$, slightly lower than what is observed. The ion $C_2H_7O_2^+$ (*m*/*z* 63) is oversaturated and therefore its occurrence is unlikely, although its presence may contribute to the $^{13}C_2H_5O_2^+$ peak. The ^{13}C isotope patterns of all other polyatomic ions were difficult to distinguish due to the presence of radical cations at even mass/charge ratios in the ICP mass spectra.

A fragmentation pathway for the protonated glucose and fructose in the plasma is proposed in Scheme 3. Due to the similarity of the ICP mass spectrum of sucrose with those of the monosaccharides (Table 3), it is assumed that there is

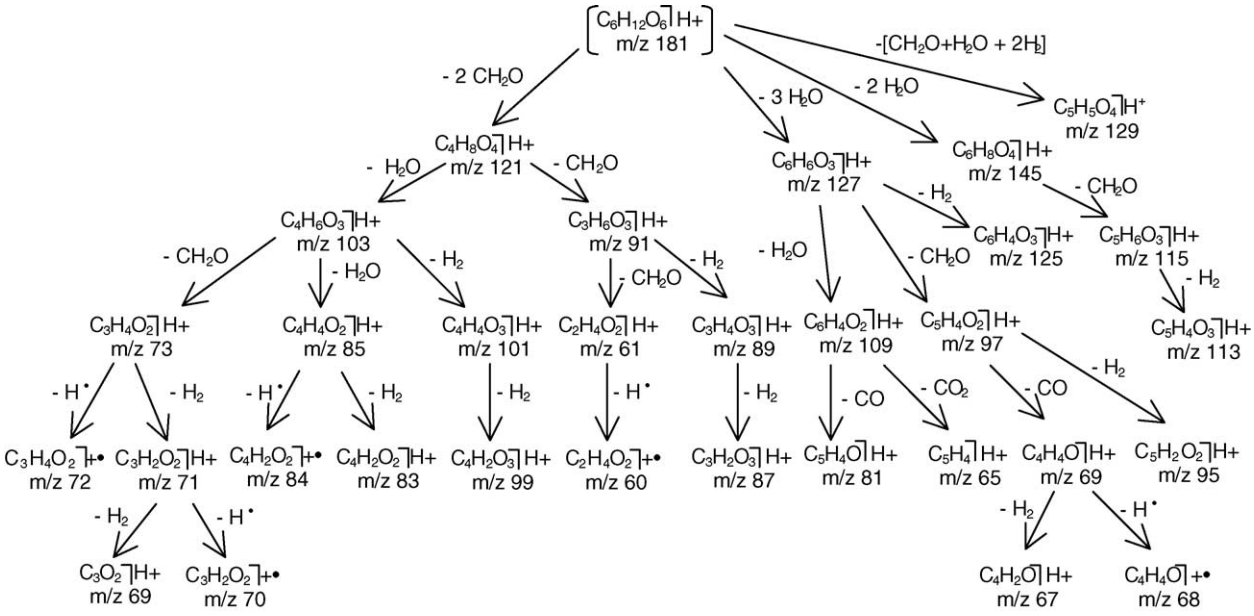

Scheme 3. Proposed fragmentation scheme of protonated glucose and fructose to form the major polyatomic ions observed in mass spectra of glucose and fructose obtained by ICP-MS. Elemental compositions shown in square parenthesis were not observed.

facile scission of the glycoside bond of the sucrose molecule to produce glucose and/or fructose, as was observed in the ESI-MS/MS spectrum (Fig. 8). The similarity of the fructose, glucose, and sucrose ICP mass spectra is explained by the molecules fragmenting to form common intermediates at *m*/*z* 121, 127, and 145, which then undergo further decomposition to produce the other ions present in the spectrum; the only exception being the ion at *m*/*z* 129, which is formed by four neutral losses from both the fructose and glucose molecules, with none of the intermediate ions observed. As with the ESI-MS/MS spectra, neutral losses of H_2O and CH_2O, having exothermic heats of formation of −116 and −242 kJ/mol, respectively, occur frequently in the fragmentation scheme. Neutral loss of H_2 ($\Delta H_f = 0$ kJ/mol) was also observed in the formation of the highly unsaturated fragment ions in the ICP mass spectra. This type of oxidation reaction is observed in higher energy systems, and appears to take place in the ICP. The moieties at *m*/*z* 81 and 65 are formed by loss of CO and CO_2 from a larger fragment ion (*m*/*z* 109), and again, heats of formation of these neutral molecules are exothermic ($\Delta H_f(CO) = -26$ kJ/mol and $\Delta H_f(CO_2) = -94$ kJ/mol).

The corresponding protonated form to the deprotonated product ions of *m*/*z* <130 observed in the ESI mass spectra were observed also in the ICP mass spectra together with many other ions of lower mass/charge ratio. The protonated species at *m*/*z* 163 and 151, corresponding to the ions at *m*/*z* 161 and 149, respectively, observed in the ESI-MS/MS spectra, were not observed in the ICP spectra. The absence of ions at *m*/*z* 163 and 151 demonstrates that the higher energy of the plasma causes the sugar molecules to undergo more fragmentation than in the lower energy collision induced dissociation (CID) processes of ESI-MS/MS. The ESI-MS/MS spectrum of fructose provided a good source of comparison because this molecule produced a large number of collision products and was subjected to higher collision energies.

Formation and structure of the moiety at *m*/*z* 121 from glucose and fructose is proposed in Scheme 4, where loss of two formaldehyde molecules causes rearrangement of the 6-membered glucose ring to a 5-membered ring, as was also suggested by the ESI-MS/MS spectrum of glucose (Scheme 2). Further fragmentation of the positively charged ion at *m*/*z* 121 by dehydration is shown to form two possible structures of the ion present at *m*/*z* 103. The 4,5-dihydroxyfuran form of the ion at *m*/*z* 103 then undergoes dehydration to form the moiety at *m*/*z* 85, or loses CH_2O to form the protonated 4-membered ring at *m*/*z* 73. The corresponding deprotonated molecules of the ions at *m*/*z* 73 and 101 are present also in the ESI-MS/MS spectrum of fructose, for which a similar formation pathway is proposed. In the ICP mass spectrum, neutral losses of H_2 and radical H from the ions at *m*/*z* 73 and 85 form the highly unsaturated ions at *m*/*z* 69 through 72, and 84 and 83, respectively. The 4-membered rings and multiple double bonds in these structures may cause them to be resilient to further degradation in the plasma, thus explaining the relatively high intensities observed for these ions. The 2,5-dihydroxyfuran form of the ion at *m*/*z* 103 also undergoes two consecutive losses of H_2, to form the ions at *m*/*z* 101 and 99.

Loss of CH_2O from the moiety of *m*/*z* 121 requires ring rearrangement to a 4-membered ring of *m*/*z* 91. This fragment undergoes two consecutive losses of H_2 to from the ions at *m*/*z* 89 and 87. The corresponding deprotonated molecules to ions present at *m*/*z* 91 and 89, (that is, negative ions *m*/*z* 89 and 87) were present also in the ESI-MS/MS spectrum of fructose, and the formation of the ion at *m*/*z* 87 was the only loss of H_2 observed in the ESI product ion mass spectrum.

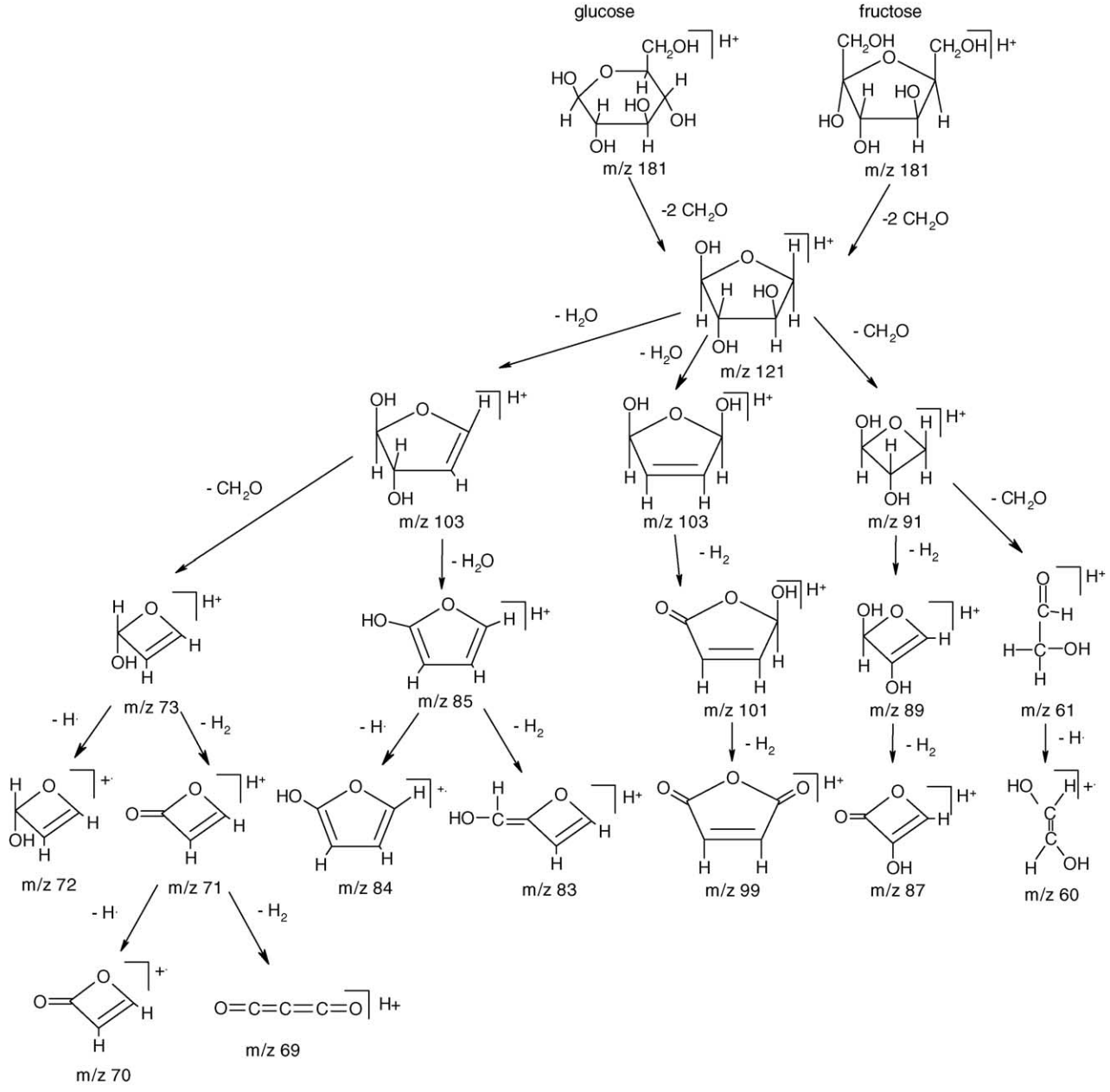

Scheme 4. Proposed formation, structure, and fragmentation of *m/z* 121 observed by ICP-MS from protonated fructose and glucose molecules.

It is presumed, therefore, that such an oxidative reaction is more likely to proceed in the higher energy of the plasma ion source than in CID of electrospray-generated ions.

The moiety at *m/z* 91 also undergoes loss of CH_2O to form the aldehyde ion at *m/z* 61 (Scheme 4). Formation of the radical cation at *m/z* 60 is then facilitated by loss of a hydrogen atom to produce $C_2H_4O_2^+$.

The protonated glucose and fructose molecules also undergo loss of two and three H_2O molecules to form both furan and pyran forms of the ions at *m/z* 127 and 145, respectively (Scheme 5). Both forms of ion at *m/z* 127 undergo oxidative loss of H_2 to form the furan species at *m/z* 125. The species at *m/z* 127 also undergo further dehydration, resulting in ring cleavage to form the acid and ketone species at *m/z* 109. The acid species at *m/z* 109 undergoes loss of CO_2 to form the moiety at *m/z* 65, and the ketone at *m/z* 109 undergoes loss of CO to form the ion at *m/z* 81.

The furan and pyran forms of the ion at *m/z* 145 undergo loss of CH_2O to form the species at *m/z* 115. The corresponding deprotonated ions to *m/z* 145 and 115, those being *m/z* 143 and 113, were observed in both fructose and glucose ESI-MS/MS spectra (Schemes 1 and 2), providing further agreement between fragment ions formed in the ICP with those formed in ESI-MS/MS. Loss of H_2O from the ion at *m/z* 115 results in ring collapse to the form the moiety at *m/z* 97. This ion undergoes facile loss of CO to form the ion

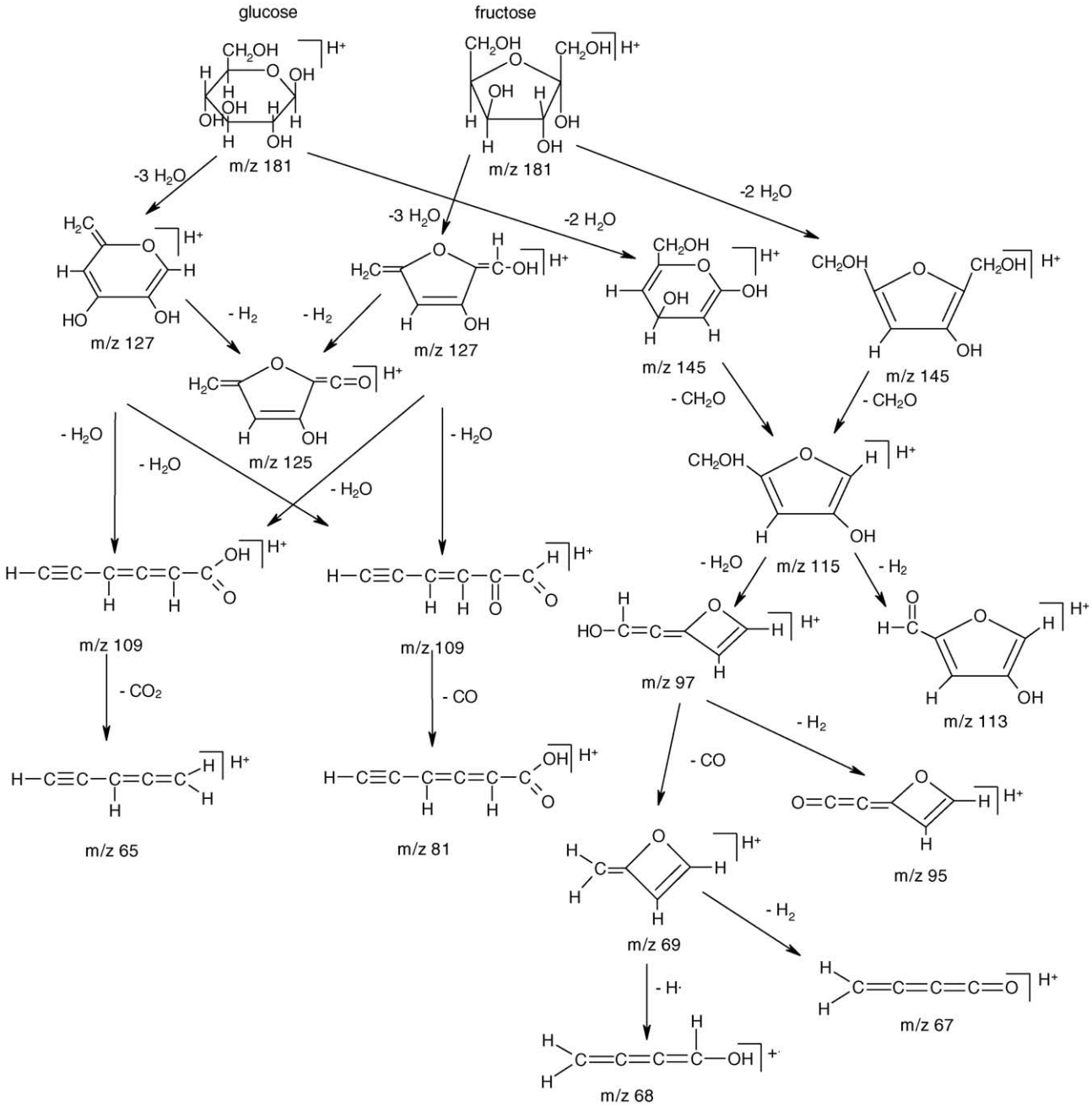

Scheme 5. Proposed formation, structure, and fragmentation of *m/z* 127 and 145 observed by ICP-MS from protonated fructose and glucose molecules.

at *m/z* 69, which in turn loses H_2 and radical H to form the ions at *m/z* 68 and 69, respectively. Oxidative losses of H_2, observed throughout the ICP spectra, form the highly unsaturated ions at *m/z* 113 and 95, from the moieties at *m/z* 115 and 97, respectively.

4. Conclusions

The presence of large polyatomic ions in the ICP mass spectra of solutions with a high sugar content, but not in solutions of ethanol or acetic acid having similar concentrations of C, H, and O and densities of similar chemical bonds, is explained by the incomplete atomization of the solute in the plasma due to combined effects of the ring structure of the solute and insufficient residence time in the plasma. Both ICP mass spectra and ESI-MS/MS product ion mass spectra of sugar solutions show fragmentation pathways involving neutral losses of CH_2O and H_2O. However, with an ICP source, these fragmentation pathways are accompanied by fragmentation pathways of higher activation energy that involve neutral losses of CO, CO_2, H_2, and hydrogen atoms.

The presence of polyatomic ions in ICP mass spectra accentuates the necessity for careful consideration of sample matrix in analysis of real samples by ICP-MS.

Acknowledgements

The authors acknowledge the financial support from the Natural Sciences and Engineering Research Council of Canada (Discovery Grants Program), the Canada Foundation for Innovation, the Ontario Research & Development Challenge Fund and Trent University.

References

[1] J.D. Douglas, S.D. Tanner, in: A. Montaser (Ed.), Inductively Coupled Plasma Mass Spectrometry, Wiley-VCH, New York, 1998, p. 620.
[2] R.S. Houk, N. Praphairaksit, Spectrochim. Acta B 56 (2001) 1069 (and references therein).
[3] B. Hattendorf, D. Gunther, Fresenius J. Anal. Chem. 370 (2001) 483.
[4] S.H. Tan, G. Horlick, Appl. Spectrosc. 40 (1986) 445.
[5] H.P. Longerich, J. Anal. At. Spectrosc. 8 (1993) 439.
[6] V.F. Taylor, Trace element fingerprinting of canadian wine, M.Sc.Thesis, Memorial University of Newfoundland, St. John's, NF, 2001.
[7] V.F. Taylor, H.P. Longerich, J.D. Greenough, J. Agric. Food Chem. 51 (2003) 856.
[8] M.J. Baxter, H.M. Crews, J. Dennis, I. Goodall, D. Anderson, Food Chem. 60 (1997) 443.
[9] M.M. Castineira, R. Brandt, A. von Bohlen, N. Jakubowski, Fresenius' J. Anal. Chem. 370 (2001) 553.
[10] K. Danzer, D. De La Calle Garcia, G. Thiel, M. Reichenbacher, Amer. Lab. 31 (1999) 26.
[11] C. Marisa, R. Almeida, M. Teresa, S.D. Vasconcelos, M. Barbaste, B. Medina, Anal. Bioanal. Chem. 374 (2002) 314.
[12] M.Y. Perez-Jordan, J. Soldevila, A. Salvador, A. Pastor, M. Guardia, J. Anal. At. Spec. 13 (1998) 33.
[13] R.E. March, C.J. Stadey, Rapid Commun. Mass Spectrom. (2005), in press.
[14] Y. Cai, M.C. Concha, J.S. Murray, R.B. Cole, J. Am. Soc. Mass Spectrom. 13 (2002) 1360.
[15] J.H. Zhu, R.B. Cole, J. Am. Soc. Mass Spectrom. 12 (2001) 1193.
[16] W. Chai, V. Piskarev, A.M. Lawson, Anal. Chem. 73 (2001) 651.
[17] N.G. Karlsson, B.L. Schulz, N.H. Packer, Am. Soc. Mass Spectrom. 15 (2004) 659.
[18] O.M. Saad, J.A. Leary, Anal. Chem. 75 (2003) 2985.
[19] C. Thanawiroon, K.G. Rice, T. Toida, R.J. Linhardt, J. Biol. Chem. 279 (2004) 2608.
[20] W. Wu, C. Yan, L. Li, Z. Liu, S. Liu, J. Chromatogr. A 1047 (2004) 203.
[21] X.S. Miao, C.D. Metcalfe, C.Y. Hao, R.E. March, J. Mass Spectrom. 37 (2002) 495.
[22] R.E. March, X.S. Miao, C.D. Metcalfe, M. Stobiecki, L. Marczak, Int. J. Mass Spectrom. 232 (2004) 171.
[23] F. Cuyckens, R. Rozenberg, E. de Hoffmann, M. Claeys, J. Mass Spectrom. 36 (2001) 1203.
[24] F. Ferreres, R. Llorach, A. Gil-Izquierdo, J. Mass Spectrom. 35 (2004) 312.
[25] M.P. Dziewatkoski, L.B. Daniels, J.W. Olesik, Anal. Chem. 69 (1996) 1101.
[26] S.E. Hobbs, J.W. Olesik, Spectrom. Chim. Acta B 52 (1997) 353.
[27] R.S. Jackson, Wine Science: Principles and Applications, Academic Press, Toronto, 1994.
[28] I. Rodushkin, F. Odman, P.K. Appelbad, J. Food Comp. Anal. 12 (1999) 243.
[29] M. Ben-Younes, D.C. Gregoire, C.L. Chakrabarti, Spectrochim. Acta B 58 (2003) 361.
[30] C. Duyck, N. Miekeley, C.L. Porto do Silveira, P. Szatmari, Spectrochim. Acta B 57 (2002) 1979.
[31] D. Hausler, Spectrochim. Acta B 42 (1987) 63.
[32] J. Zhang, J.S. Brodbelt, J. Am. Chem. Soc. 126 (2004) 5906.
[33] E.P. Hunter, S.G. Lias, J. Phys. Chem. Ref. Data 27 (1998) 413.